Fountain Journal of Natural and Applied Sciences 2023; 12(2): 55-74

DOI: 10.53704/fujnas.v12i2.438

A publication of College of Natural and Applied Sciences, Fountain University, Osogbo, Nigeria.
Journal homepage: www.fountainjournals.com
ISSN: 2354-337X(Online),2350-1863(Print)

Optimization of Adsorption Potentials of Nigerian Kaolinite Mineral Through Acid Activation

[1*]Abu, T. O., [2]Adegoke, H. I. and [3]Odebunmi, [c]E. O.

[1]Department of Industrial Chemistry, University of Ilorin, Ilorin, Nigeria
[2]Department of Chemistry, University of Ilorin, Ilorin, Nigeria
[3]Department of Chemistry, Thomas Adewumi University, Oko, Nigeria

Abstract

The adsorption capacities of Nigerian Kaolinite minerals obtained from Share in Kwara State in raw and acid-activated forms towards some heavy metal ions were evaluated. The clay mineral was purified by sedimentation method and modified with 0.1M nitric, sulphuric, phosphoric, acetic, and oxalic acids. The properties of the raw clay and the effects of acid activation were investigated by X-ray diffraction (XRD), Scanning electron microscopy (SEM), Fourier-Transform infrared spectroscopy (FTIR) and BET surface area analyses. Adsorption and desorption studies were subsequently carried out to evaluate the efficiencies of clay samples in removing Pb^{2+}, Cd^{2+} and Ni^{2+} ions from aqueous solutions. Effects of operation parameters viz pH, initial concentration, temperature, and time on the adsorption process were determined on the raw samples, and optimum conditions obtained were utilized for evaluation on the acid-activated samples. The acid modification was found to achieve considerable leaching of exchangeable cations on the clay mineral as confirmed by variations of the d-spacings, lowering of peak intensities and changes in absorption bands of the acid-modified samples (A-K (Acetic acid-Kaolinite), N-K (Nitric acid-Kaolinite), O-K (Oxalic acid-Kaolinite), P-K (Phosphoric acid-Kaolinite) and S-K (Sulphuric acid-Kaolinite). The surface areas increased in S-K, O-K and especially N-K (162.227 m^2/g) from 114.9457 m^2/g [Raw Kaolinite (R-K)] to) but reduced in A-K 112.865 m^2/g and P-K (113.872 m^2/g). The activated clay samples were found to adsorb higher amounts of all the heavy metal ions studied than the raw form of the clay. Desorption analysis results revealed that the clay mineral can be regenerated and reused. Compared with other methods, modification with dilute acid provides a simple, effective, and environmentally friendly method of improving the surface characteristics of clay minerals to enhance their adsorption capacities as suitable adsorbents for water remediation purposes.

Keywords: Bentonite, Kaolinite, Adsorption, Heavy metals, Desorption

Introduction

Recent technological advances have resulted in corresponding improvements in several areas of human existence. However, this has also placed lots of constraints on the ecosystem as wastes generated from activities to sustain and improve our lives are discharged indiscriminately into the environment, especially the water environment.

*Corresponding Author: + 2349096380975
Email: abu.to@unilorin.edu.ng

A major component of such wastes are heavy metals, which enter the water environment through industrial activities such as mining, refining, electroplating, storage cells, metal smelting and finishing, engine exhausts, industrial effluents, sludge, etc. (Huang *et al.,* 2020; Dim *et al.,* 2021; Aziz *et al.*, 2023)

Industrial wastewater has been shown to contain heavy metal ions such as cadmium, nickel, chromium, and lead (Berihun & Solomon, 2017; Aziz *et al.*, 2023). These metals have been established as hazardous pollutants due to their non-biodegradability, bioaccumulation, and carcinogenic tendencies. As such, it is necessary to remove them from industrial wastewater before their discharge into the water environment (El-Naggar *et al.*, 2019; Khalfa *et al.,* 2020; Balali-Mood *et al.*, 2021). To achieve this, several wastewater treatment techniques have been proposed, out of which adsorption is the most efficient due to the low costs of design and operation (Uddin, 2017; Dim et al., 2021; Malima *et al.,* 2021).

Several materials have been used as potential adsorbents for removing heavy metals from wastewater. However, significant attention has been drawn to naturally occurring clay minerals because of their natural availability and abundance. (Fernandes *et al.*, 2020, Khalfa *et al.,* 2020). Previous studies have confirmed the favourable adsorption of metal ions on clay minerals (Li et al., 2020; Es-said et al., 2021; Chen *et al.*, 2023). Several reagents, such as inorganic and organic acids and alkaline as well as organic salts, have been used to modify the surfaces of clay adsorbents (Kumar et al., 2013; Lawal et al., 2020; Budash *et al.*, 2023). This is because the modification of clay minerals allows the removal of impurities and improvement of the silica-to-alumina ratio as well as surface area (Emam et al., 2016; Bennour, 2017; Kakaei et al., 2020; Budash *et al.*, 2023).

Although numerous studies have been conducted on the adsorption of heavy metal ions on clay surfaces, there is still the need for continued investigations to derive sufficient empirical data to adequately model adsorption systems involving these minerals to maximise their benefits as suitable adsorbents for water remediation purposes. In addition, most previous studies on acid activation of clays involved using concentrated strong acids, which has sometimes raised environmental concerns; thus, it is necessary to test if diluted strong or weaker organic acids could be suitable alternatives.

In this study, locally sourced Kaolinite mineral was purified and subsequently modified with (0.1M) nitric, sulphuric, phosphoric, acetic, and oxalic acids. The raw and modified adsorbents were characterized by Fourier Transform Infra-red (FTIR), X-ray Diffractogram (XRD), and Scanning Electron Microscope (SEM), as well as BET surface area analysis. The adsorption of three heavy metal ions (Pb^{2+}, Cd^{2+} and Ni^{2+}) from their respective aqueous solutions using the raw and acid-activated forms of the clay was subsequently investigated. Desorption analysis was also investigated on the raw clay adsorbent.

Materials and Methods

Materials

The chemical reagents that were used include Nickel sulphate ($NiSO_4 \cdot 6H_2O$ Molecular weight 154.76g/mol, 99.99%); Cadmium sulphate ($CdSO_4 \cdot 8H_2O$; Molecular weight 208.47g/mol, 99.99%); Lead nitrate ($Pb(NO_3)_2$; Molecular weight 331.21g/mol, 99.0%); Nitric acid (HNO_3; Molecular weight 63.01g/mol, 90%); Phosphoric acid (Molecular weight 98.00g/mol, 85%); Hydrochloric acid (Molecular weight 36.46g/mol, 37%); Sodium hydroxide (Molecular weight 40.0g/mol, 98%); Acetic acid (Molecular weight 60.05g/mol, 98%) and Oxalic acid (Molecular weight 90.03g/mol, 85%). All reagents were of analytical grade and obtained from Sigma Aldrich, USA and BDH, United Kingdom.

Purification of Kaolinite Clay Mineral

The clay sample was purified by adopting and modifying the method previously described (Ho *et al.*, 2001; Bhatt *et al.*, 2012), which involved the addition of 500 ml of de-ionized water to 10 g clay. The resulting suspension was left to swell for 24 h after which it was subjected to manual stirring with a wooden rod for 30 min and left for 4 hrs to allow sedimentation of the impurities. The clay was recovered through decantation and centrifuged

using (KUBOTA-6500) at 4000 rpm for 20 min. The recovered clay was then dried at 80 ˚C, ground, labelled and stored in airtight sample bottles. This was done severally until considerable amounts of the clay had been purified.

Acid Activation

A modified method earlier described in Literature (Özcan & Özcan, 2004; Akpomie & Dawodu, 2016;) was also adopted. A 50 g sample of purified clay mineral was suspended in 250 ml of 0.1 M acid in a 500 ml beaker and stirred for 30 min, after which it was allowed to stand for 24 hrs at room temperature. The settled mixture was then decanted, and the resulting clay slurry was washed thoroughly with de-ionized water until pH 7 was attained. The moist clay was heated in an oven at 105 ˚C for 2 hrs to obtain dried acid-activated clay, which was appropriately labelled and stored.

Characterization of Raw and Acid-Activated Clays

Mineralogical compositions of the clays were determined through measurements using a multipurpose X-ray diffractometer D8-Advance from Bruker operated in a continuous ϑ-ϑ scan in locked coupled mode with Cu-K_α radiation at i-Themba Labs, South Africa. The physical surface morphologies of the raw and acid-activated forms were observed through SEM/EDX analysis using a Zeiss Merlin Microscope at the Massachusetts Institute of Technology (MIT), USA. At the same time, Fourier Transform Infrared (FTIR) spectra were obtained with Shimadzu IR Affinity-1S spectrophotometer using the mull technique at the University of Cape Town, South Africa. The surface areas of the clay samples were determined through Nitrogen adsorption/desorption isotherms at -196˚C measured on a Micromeritics Tristar 3020 Porosimeter available at the University of Cape Town, South Africa. The total specific surface area (S_{BET}) was evaluated by the Brunauer-Emmet-Teller (BET) method while the micropore volume was determined through the t-plot method. The total pore volume was calculated at the relative pressure p/p_0 of 0.97, and the micropore volume was determined by the t-plot method. The pore size distribution was evaluated through the Barrett-Joyner-Halenda (BJH) method.

Adsorption Analysis

Stock solutions of lead, nickel and cadmium ions were prepared by dissolving the desired amount of the metal salt ($Pb(NO_3)_2, NiSO_4 \cdot 6H_2O, 3CdSO_4 \cdot 8H_2O$ in an appropriate volume of deionized water. A 100 ml of varying concentrations (10-250 mg/L) of metal solution (Lead, chromium, nickel in turns) was poured into conical flasks, and the pH of the solutions was adjusted (2 to 4.5 for Pb and 2-7 for Ni and Cd) using dilute nitric acid (HNO_3) and sodium hydroxide (NaOH) when necessary. Then 40 mg of raw kaolinite clay was added into each, after which the flasks were placed in a rotary shaker at 250 rpm at the desired conditions of temperature$30 - 60^oC$, and time (10 min – 3.5h). After shaking, the contents of the flasks were centrifuged at 3000 rpm for 20 min and then filtered. Atomic Absorption Spectroscopy determined the residual concentrations of the metals in the supernatant solutions. The AAS was recorded on a Buck 200 atomic absorption spectrophotometer at ROTAS Soil Lab Limited, Ring Road, Ibadan, Nigeria.
The quantities of the metals adsorbed were determined using the equation below.

$$q_e = \frac{C_o - C_e}{m} \text{ x } V \quad (1)$$

where q_e is the amount of metal adsorbed (mg/g)
C_o is the initial concentration of the metal in the aqueous solution (mg/L)
C_e is the concentration of the ions at the equilibrium stage (mg/L)
m is the mass of the adsorbent (g)
V is the volume of metal solution used (L)

Adsorption Isotherms

The experimental data obtained from the investigation of the effects of initial concentration on the adsorption of the heavy metal ions were evaluated with various adsorption isotherm models to explain the equilibrium relationship between the adsorbent and adsorbate as well as determine the maximum adsorption capacities of the adsorbents (Akpomie & Dawodu, 2016; Pathania *et al*., 2017;

Omer *et al*., 2018). The isotherm models: Langmuir, Freundlich and Dubinin-Radushkevich, were tested for their compatibilities with the adsorption data.

Langmuir Adsorption isotherm

For Langmuir isotherm, the linearized form of the equation was used for the evaluation as presented thus:

$$\frac{C_e}{q_e} = \frac{1}{q_m C_e} + \frac{1}{K_a q_m} \quad (2)$$

where C_e represents the equilibrium concentration of the substrate (mg. L-1), qe is solid phase concentration (mg/g), qm (mg/g), and Ka (L/mg) are empirical constants that were evaluated from the slope and intercept respectively of the plot of Ce/qe against Ce. (Do, 1998; Hamdaoui & Naffrechoux, 2007; Foo & Hameed, 2010)

Freundlich Adsorption Isotherm

The linear form of the isotherm is represented thus:

$$lnq_e = lnK_f + \frac{1}{n} lnC_e \quad (3)$$

lnq_e was plotted against ln C_e, and the values of n (the heterogeneity factor of sorption) and K_f (the Freundlich adsorption constant ($mg^{1-(1/n)}\ L^{1/n}\ g^{-1}$ were obtained from the slope and intercept respectively (Hamdaoui & Naffrechoux, 2007; Foo & Hameed, 2010, Bahl *et al.*, 2012;)

Dubinin-Radushkevich Adsorption Isotherm Model

The linearized form of the isotherm model is given as:

$$lnq_e = lnq_s - k_{ads}\varepsilon^2 \quad (4)$$

where ε is Polanyi potential and is given as [RTln(1+ 1/Ce)], a plot of ln qe against ε^2 was drawn, and the values of k_{ads}, a constant related to mean free energy of adsorption per mole of the adsorbate ($mol^2/k\ J^2$) and q_s (the theoretical saturation capacity (mg g^{-1}) were obtained from the slope and intercept respectively (Do, 1998; Foo & Hameed, 2010).

Kinetics Studies of Adsorption Data

The experimental data was tested with four kinetic models viz Pseudo first order, Pseudo second order, Elovich and Intra-particle diffusion through the appropriate plots to determine the values of calculated parameters. The model whose calculated as well as experimental values agree and has a correlation coefficient R2 much closer to unity was used to determine the controlling mechanism of the sorption process (Sukpreabprom et al., 2014; Akpomie & Dawodu, 2016; Pathania et al., 2017; Omer *et al*., 2018).

(i) Pseudo First-Order Model

The linearized Lagergren's equation was used to test for pseudo-first-order kinetics:

$$log(q_e - q_t) = \log q_e - \frac{k_1}{2.303} t \quad (6)$$

where qe and qt are adsorption capacities at equilibrium and at time t, respectively (mg. g-1), and k1 is the rate constant of pseudo-first-order adsorption (min^{-1}) (Abechi *et al*., 2011). log ($q_e - q_t$) versus t was plotted to determine the values of k_1 as well as q_e from the slope and intercept respectively (Abechi *et al*, 2011; Boparai *et al*., 2011).

(ii) Pseudo Second Order Model

The pseudo-second-order rate expression is linearly expressed as (Ho & Mckay, 1998; Boparai *et al*, 2010):

$$\frac{t}{q_t} = \frac{1}{k_2 q_e^2} + \frac{1}{q_e}(t) \quad (7)$$

The plot of (t/qt) against t was drawn from which the values of q_e and k_2 were determined from the slope and intercept of the plot, respectively (Ho & Mckay,1998; Boparai et al., 2010; Abechi et al., 2011).

(iii) Elovich Model

The Elovich kinetic model was also tested using the following linearized equation:

$$q_t = \frac{1}{\beta} ln(\alpha\beta) + \frac{1}{\beta} lnt. \quad (8)$$

The term q_t was plotted against lnt to obtain a straight line where the values of β and α were determined from the slope and intercept, respectively (Ramachandran *et al.*, 2011)

(iv) Intra-particle Diffusion Model

The data was further correlated with an intra-particle diffusion model of the form:

$$qt = Kt_{1/2} + Ci \quad (9)$$

In this case, it was also plotted against t1/2, and K and C were obtained from the straight-line plot. (Ramachandran *et al*, 2011)

Thermodynamic Studies of the Adsorption Process

For thermodynamic studies, parameters such as free energy change (ΔG_{ads}), standard enthalpy change (ΔH_{ads}) and standard entropy change (ΔS_{ads}) were estimated from the adsorption data using the following equations (Boparai *et al.*, 2011; Al-Anber, 2011):

$$lnK = \frac{\Delta S}{R} - \frac{\Delta H}{RT} \quad (10)$$

$$\Delta G = \Delta H - T\Delta S \quad (11)$$

Substitution of equation 10 into 11 yields the vant' Hoff equation (Levine, 2009; Omer *et al*., 2018):

$$\Delta G = -RTlnK \quad (12)$$

K was calculated as follows:

$$K = \frac{q_e}{C_e} \times M_{adsorbate} \times C \quad (13)$$

q_e is the amount of dye adsorbed per unit mass of the clay, C_e is the equilibrium metal concentration (mg L^{-1}), M is the molecular weight of the adsorbed species, and C is the concentration of the solution in the chosen standard state (Omer *et al*., 2018). The lnK values obtained at the investigated temperatures were plotted against 1/T. The thermodynamic parameters (ΔH_{ads}) as well as (ΔS_{ads}) were obtained from the slope and intercept, respectively, while (ΔGads) was found by using equation 10 at the different temperatures (Sukpreabprom et al., 2014; Akpomie & Dawodu, 2016; Pathania *et al.*, 2017; Omer *et al*., 2018).

Desorption Studies

Batch adsorption experiments were carried out by contacting 40 mg of the adsorbent with 100 ml of metal solution (the three metals in turns) at the established optimum conditions of all the factors investigated for 30 min in triplicates. The residual adsorbents after separation were rinsed mildly with de-ionized water in a flask to remove any un-adsorbed substrate, after which 25 ml of 0.5M NaOH, 0.5M HCl and de-ionized water were added to each residue. The mixture was stirred for 2 hrs after which separation was done by centrifuging at 3000 rpm for 20 min and subsequent filtration. The amount of substrate desorbed in the supernatant was determined by AAS (Ewere *et al.*, 2014; Chen & Zhao, 2009; Likita *et al.*, 2016; Siyanbola *et al.*, 2011). The percentage of desorbed metal ions was calculated using the equation below:

$$K_d = \frac{C_o}{C_a} \text{ X } 100 \quad (14)$$

where K_d is the amount of desorbed metal ions, C_o is the concentration of desorbed metal ion, and C_a is the concentration of adsorbed metal ion.

Results and Discussions

Characterization of Natural and Acid Activated Kaolinite

XRD Analysis Results of Raw and Acid-Activated Kaolinite

The XRD spectrum of the raw kaolinite clay presented in Figure1a shows that the only crystalline phase in the sample is kaolinite which indicates high level of purity of the sample as other crystalline phases like quartz and mica were not identified (Hai, et. al, 2015). Figure 1b Compared view of the raw and acid-activated clays.

The kaolinite mineral is identified by peaks at 2θ positions (12.34, 19.82, 24.8, 38.38 and 61.96). The two crystalline peaks exhibited at 12.34° and 24.86° attributed to its (001) and (002) planes, respectively, confirm its crystalline nature, which correlates with earlier reports (Kumar & Lingfa, 2020; Moretti et al., 2020; Tian *et al.*, 2022). Compared with the raw in Figure 1b, the acid-activated forms maintained the structure and crystallinity of the clay with only slight variations in the intensities of the identifying peaks of

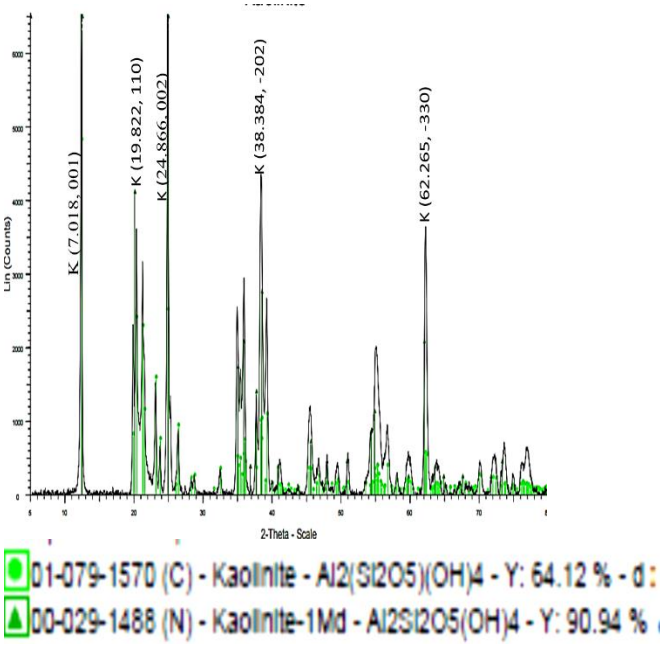

Figure 1a: XRD spectrum of R-K

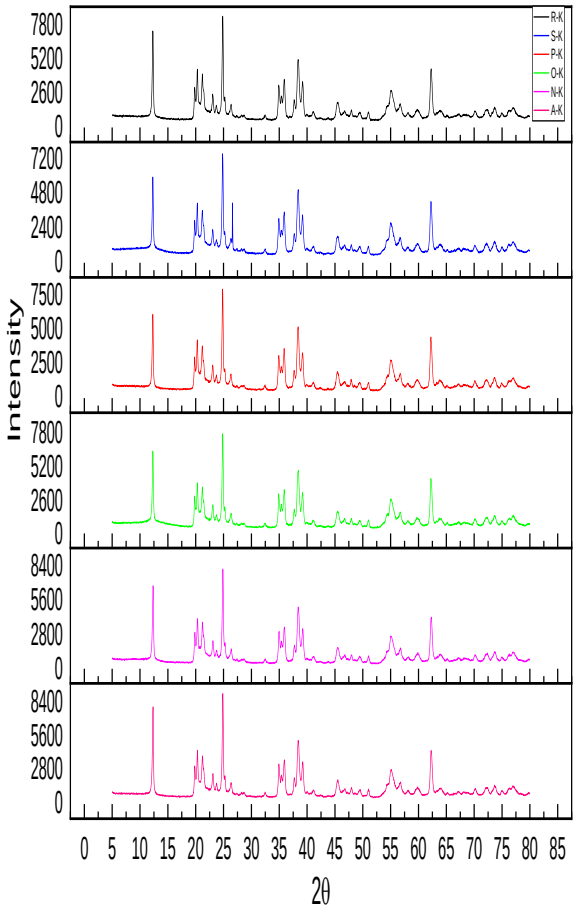

Kaolinite. This indicates de-crystallization of the clay during acid treatment and confirms the interaction of the acids with the surface of the clay (Novakovic et al., 2008; Maged *et al.*, 2020). Reduction in intensity has previously been found to be highly influenced by the strength of the acid (Kumar *et al*., 2013), and this was also the case in this study, as the trend was found to be S-K > N-K > PK ~ OK > AK.

Scanning Electron Microscopy (SEM) Results

The physical surface morphology of the raw kaolinite mineral was observed and compared with those of the acid-activated forms. As presented in Figure 2a, the raw kaolinite mineral shows highly crystallized flake-shaped clay particles arranged in clusters that coalesced to form a giant aggregate infused with large pores resembling labyrinths. The images of the acid-activated kaolinite clays, however, present the breakdown of the structure into different forms depending on the acid. The surface of A-K clay shows a porous structure of non-uniform-sized particles that are aggregated in some places, with some tiny particles deposited on the aggregates in contrast to the image of the raw Kaolin. The S-K clay contains particles of different shapes with non-uniform pores that are partially dispersed, which is probably the consequence of breaking down the rigid structure in the raw form. Amorphous porous surfaces exhibiting mild crystallinity and partial dispersion of the particles can be observed from the image of N-K clay. For P-K clay, rough surfaces containing non-uniform sized and highly dispersed particles permeated with tiny aggregates producing a considerable degree of porosity are observed. Acid treatment of the clay resulted in the transformation of the rigid crystalline surface structure to an amorphous one and the formation of lower-sized particles on the surface, consequently increasing the surface area and, thus, its affinity for cation uptake. Similar findings have been reported by Hooshiar et al., 2012, Hai *et al.*, 2015 and Ihekweme *et. al,* 2020.

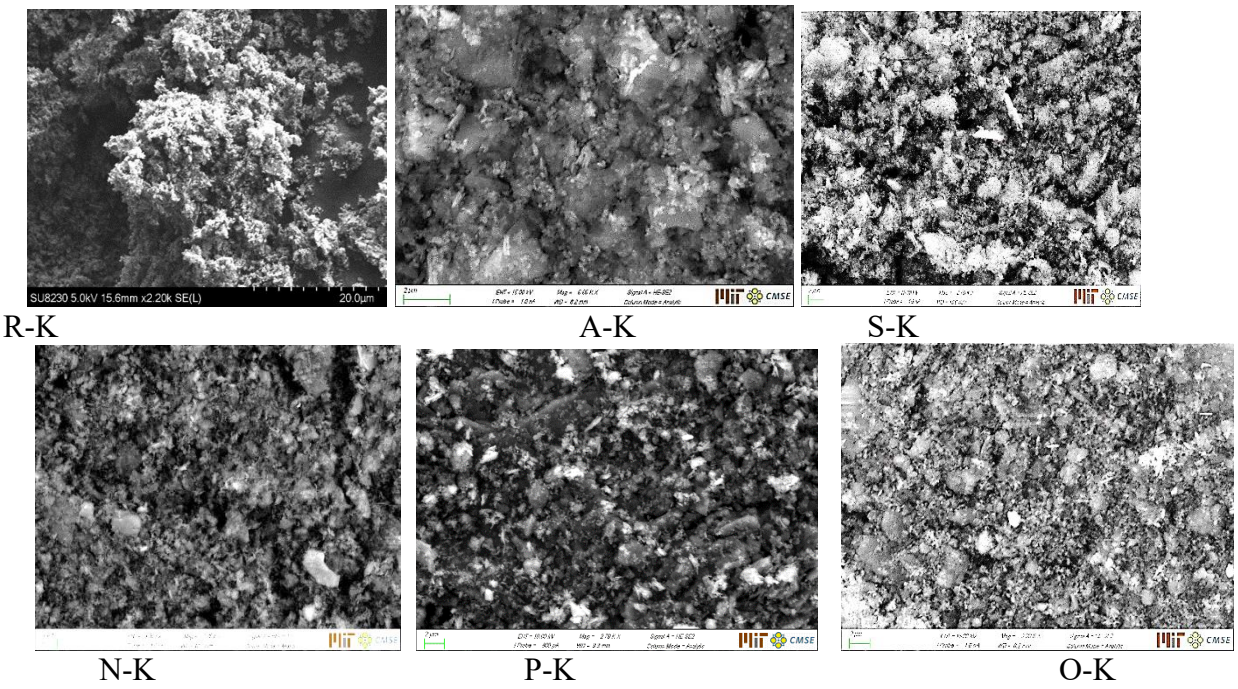

Figure 2: Scanning Electron Micrograph images of Raw kaolinite (R-K), (A-K) (S-K), (N-K), (P-K), and (O-K).

Fourier Transform Infrared Spectroscopy Analysis Results

The FTIR analysis of the raw kaolinite yielded the spectrum presented in Figure 3a, from which the functional groups were identified. The bands 3687.90, 3622.32 and 3618.46 cm^{-1} in the FTIR spectrum of R-K, as shown in Figure 3a, correspond to the inner surface –OH stretching vibrations particular to Kaolinite minerals and confirm that the clay is kaolinite (Sdiri *et al.*, 2011, Bukalo *et al.*, (2017), Alshameri *et al.*, 2018). The band at 3618.46 cm^{-1}

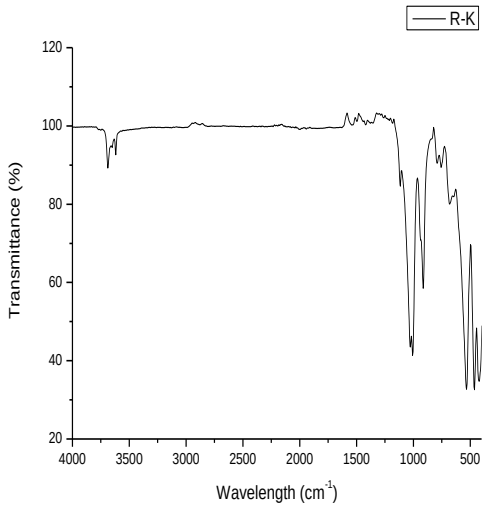

Figure 3a: FTIR spectrum of Raw Kaolinte (R-K)

is attributed to the low frequency of Kaolinite's inner – OH groups (Ihekweme *et a*l., 2020). The Si – O – Si and Al – Al – OH bands indicate OH stretching vibrations at 1006.84, 1026.13 and 1114.86 cm^{-1} and 914.26 and 790.81 cm^{-1} (octahedral sheet), respectively (Panda *et al.*, 2010, Bertagnolli & da Silva (2012), Alshameri *et al.*, 2018). The bands at 682.80 and 532.35 cm^{-1}, as well as that at 462.92 cm-1, indicate bending vibrations of Si – Al – O and Si – O – Si groups (Novakovic et al., 2008; Ozdes et al., 2011; Bertagnolli & da Silva (2012)). The functional groups identified in R-K were compared with those of the acid-activated clays, as presented in Figure 3b.

Comparison of the spectral as displayed in Figure 3b shows that the –OH stretching bands at 3687.90, 3622.32 and 3618.46 cm^{-1} were retained in acid-activated samples S-K, P-K and O-K but at reduced intensities. However, the band at 3687.90 cm^{-1} shifted to 3684.04 cm^{-1} and 3689.83 cm^{-1} in A-K and N-K respectively. The band 1114.86 cm^{-1} were retained in all the acid-activated clays but at lower intensities except for N-K, where the intensity was slightly higher. Similarly, the 1026.13 cm^{-1} was maintained in the acid-activated

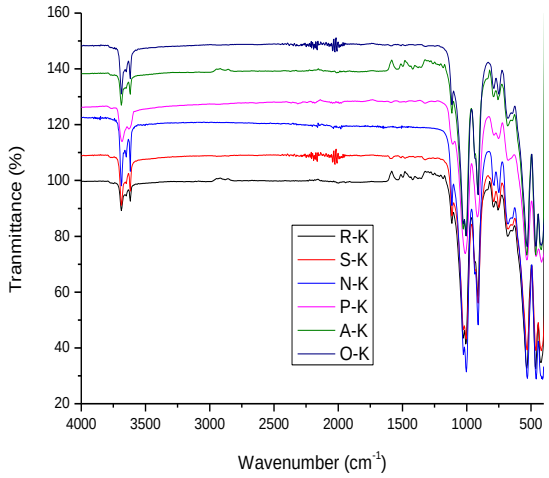

Figure 3b: Compared view of the raw and acid-activated kaolinite clays spectral

clays except N-K, which shifted to 1028.06 cm-1, while the 1006.84 cm^{-1} band was shifted to 1002.98 cm^{-1} in S-K, O-K and P-K but was preserved in A-K and N-K. The Al – Al – OH stretching vibrations at 914.26 cm^{-1} were shifted to 910.40 cm^{-1} in the trio S-K, P-K and O-K, moved to 912.33 cm^{-1} in N-K but remained in A-K at a lower intensity. A reduction in intensity was also recorded for the band 790.81 cm^{-1}, which was retained in all the acid-activated clays except in N-K, where it shifted to 788.89 cm^{-1}. The band at 682.80 cm^{-1} was still observed with higher intensity in N-K but shifted to 678.94 cm^{-1} in A-K, S-K, O-K and P-K with reduced intensities. In acid-activated clays S-K, P-K and O-K, the band 532.35 cm^{-1} band shifted to 528.50 cm^{-1} but moved to 534.28 cm^{-1} in N-K and remained in A-K. The Si – O – Si band at 462 cm^{-1} was still intact after acid treatment in all the acid-activated samples except in N-K, where it moved to 464.84 cm^{-1}.

The shift to new band positions from the initial in the raw clay and the changes in intensities of original bands in the acid-activated clays indicate the leaching of cations and de-alumination of the clay, which is expected after acid treatment. Similar findings have been reported (Novakovic *et al.*, 2008; Akpomie & Dawodu (2016), Ihekweme *et al.*, 2020).

BET Surface Area Analysis Results

The most important reason for acid modification of clay minerals is to enhance the adsorption characteristics of clay through the increase in adsorption area and void capacity. These two properties have been reported to be directly proportional to the adsorption tendency as well as the ability of the clay mineral (Sarma *et al.*,2016 & Dim *et al.,* 2021). The surface areas of the clay samples (raw and acid-activated kaolinite) determined through BET analysis along with pore volumes and sizes, are presented in Table 1. From Table 1, the surface areas of the acid-activated samples are higher than those of the raw except for A-K and P-K, where reduction occurred. The order of which is N-K (162.227 m^2/g) > S-K (151.335 m^2/g) > O-K (115.837 m^2/g)

Table 1: BET analysis result

Parameter	R-K	A-K	N-K	O-K	P-K	S-K
BET surface area, S_{BET} (m^2/g)	114.946	112.865	162.227	115.837	113.872	151.335
Langmuir surface area (m^2/g)	260.374	194.491	274.091	268.049	256.956	267.503
External specific area (m^2/g)	123.275	80.5647	141.733	115.442	112.252	132.453
Micropore area (m^2/g)	19.3005	15.452	20.4937	19.169	20.3941	20.2247
Micropore volume (cm^3/g)	0.00541	0.00617	0.00864	0.00626	0.00635	0.00706
Total pore volume (cm^3/g)	0.70588	0.51269	0.80587	0.71187	0.71213	0.80055
Pore diameter (Å)	238.767	275.606	118.424	251.387	270.418	160.338

> R-K (114.946 m^2/g) P-K (113.872 m^2/g) > A-K (112.865 m^2/g). The increase was only significant in strong acid-activated N-K and S-K, slightly so for weaker organic acid clay O-K, but reduced in the weakest acid clays P-K and A-K. The reduction in A-K and P-K surface areas occurred with an increase in their average pore diameters. Enlarging the pores after activation suggests the fixation of oxygenated groups at the opening/or on the walls of the adsorbents' micropores that could destroy the walls of the pores, thus leading to decreased surface areas. Similar reports have previously been documented in literature (Mudzielwana *et al.*, 2019; Nordin *et al.*, 2020). The total pore volume increased from R-K (0.70588 cm^3/g) to 0.80587 cm^3/g (N-K), 0.80055 cm^3/g (S-K), 0.71187 cm^3/g (O-K) and 0.71213 cm^3/g (P-K) but reduced to 0.51269 cm^3/g in A-K. There were also some changes in the pore diameter; the acid-activated clays N-K (118.424 Å) and S-K (160.338 Å) have lower diameters than R-K (238.767 Å), which is less than those of O-K (251.387 Å), P-K (270.418 Å) and the highest A-K (275.606 Å). The changes in surface area, pore volume and size of the raw clay in the acid-activated clays can be attributed to replacing exchangeable cations, generating silica, and removing impurities. All these, in no doubt, resulted in more surface creation in most of the acid-activated forms. There have been earlier reports of the enhancement of surface areas of clay minerals through acid activation (Maged *et al.*, 2020; Dim *et al.*, 2021; Malima et *al.,* 2021; Budash *et al.*, 2023)

Adsorption studies

Effect of pH

It is important to determine the effect of solution pH on the adsorption process because the pH determines the surface charge of the adsorbent, as well as the degree of ionization and speciation of the adsorbate ions (Ogbu *et al.*, 2019; Malima *et al.,* 2021). The uptake of the heavy metal ions was found to increase with an increase in pH to a

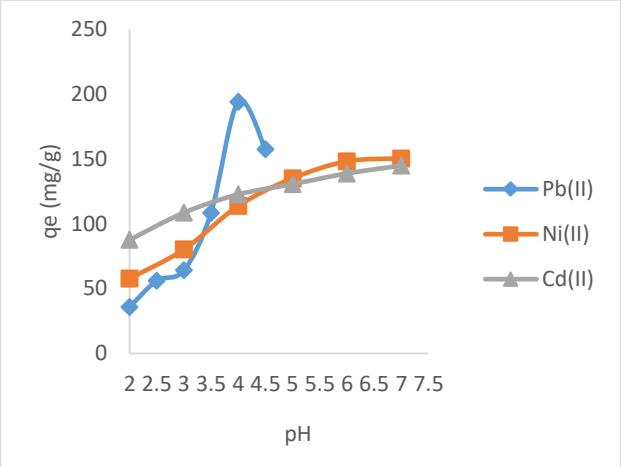

Figure 4a Effect of pH on the adsorption of heavy metal ions at 150 mg/L solutions of the heavy metals, 0.6mm particle size of the adsorbent, 0.1g of the adsorbent in 250 mL of solution, 150 rpm shaking speed, temperature of 30˚C and time, 70 mins on R-K

maximum of pH 4 for Pb^{2+} and pH 7 for Cd^{2+} as well as Ni^{2+}. Adsorption of heavy metal ions has been reported to be most effective at less acidic pH values where the competition for adsorption sites between [H_3O^+] and the positively charged heavy metal ions is minimized (Khan *et al.*, 2019; Mohamed *et al.*, 2019; Es-said *et al.*, 2021). The investigations were not extended beyond pH 4.5 and 7 for Pb^{2+} and the other two metal ions (Ni^{2+} and Cd^{2+}), respectively, because precipitations of the metals were observed beyond these values. Precipitation of metals has also been previously reported to occur at higher pH values (Dawodu & Akpomie, 2014; El-Naggar et al., 2019; Ahmadi *et al.*, 2020). Similar findings where the adsorption of the studied metals increased with increasing pH have been reported (Krika *et al.*, 2016; El-Naggar *et al.*, 2019; Chai *et al.,* 2020; Malima *et al.,* 2021),

Effect of Initial Concentration

The optimum pH values previously obtained were used while all other conditions were the same except the concentrations of the metal solutions that were varied between 10-250 mg/L. The uptake of the heavy metal ions was found to be enhanced by an increase in their initial concentrations, and this

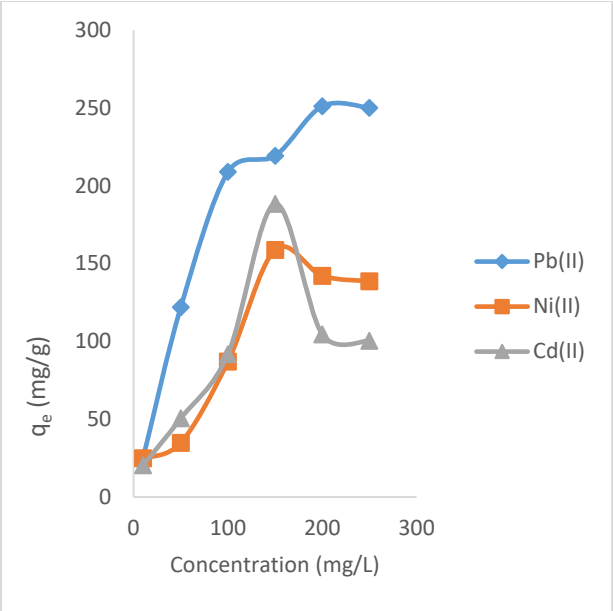

Figure 4b: Effect of initial concentration on the adsorption of heavy metal ions on Kaolinite at equilibrium

might have been a consequence of the increased concentration gradient at higher initial concentrations that can facilitate efficient mass transfer between the solid and liquid phases (Elsheik *et al.*, 2018; Mohamed *et al.,* 2019; Khalfa *et al.*, 2020). However, this occurred to a maximum of 150 mg/L for Cd2+ and Ni2+ and about 200 mg/L for Pb2+, as there were no significant increments after these concentrations. This might likely be due to saturation of the adsorbent's active sites at higher adsorbate concentrations, which could prevent further deposition of other metal ions on the adsorbent. Similar findings have been reported by Obayomi & Auta, 2019; Khalifa et al., 2020 and Nordin *et al.*, 2020.

Effect of temperature

The temperature of the adsorption experiments was varied between 303-333K to determine its effect if any. The optimum conditions obtained from the previous experiments were used. The adsorption of Pb^{2+} was found to decrease with an increase in temperature, which suggested that some amount of heat was evolved in the binding of the metal ion to the adsorbent surface, thus indicating an exothermic process. An initial increase and subsequent adsorption fall.

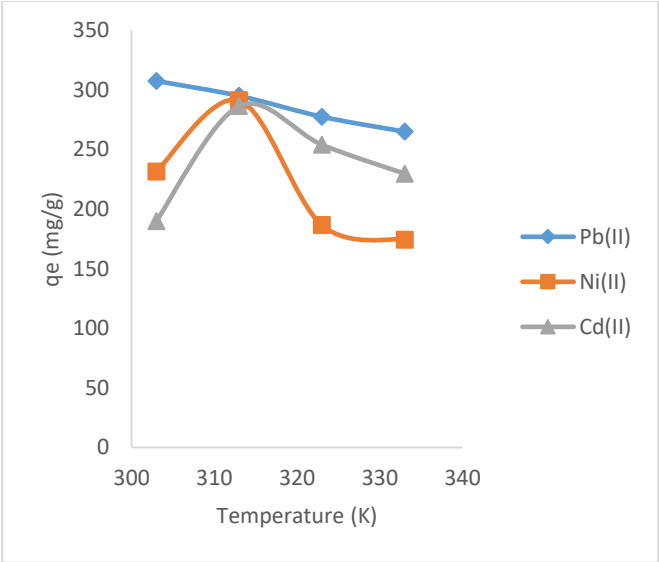

Figure 4c: Effect of temperature on the adsorption of heavy metal ions at equilibrium on Kaolinite

The temperature of the adsorption experiments was varied between 303-333K to determine its effect if any. The optimum conditions obtained from the previous experiments were used. The adsorption of Pb^{2+} was found to decrease with an increase in temperature, which suggested that some amount of heat was evolved in the binding of the metal ion to the adsorbent surface, thus indicating an exothermic process. An initial increase and subsequent adsorption fall were observed for Ni^{2+} and Cd^{2+} ions. However, the adsorption at the lowest temperature was found to be the least uptake for Cd^{2+}, suggesting an endothermic process. Similar findings have earlier been reported (Mohamed *et al.*, 2019; Chai *et al.*, 2020).

Effect of time

The effect of time on the adsorption of the heavy metal ions was investigated at 8 different time intervals within the range of 10 mins-3.5 hrs at the optimum conditions of the other parameters previously determined. The uptake of the heavy metal ions was found to be most effective at an initial time, after which a progressive decline then occurred till the end of the period investigated. This is because at initiation, the sites are empty and rapidly filled, thus resulting in an increase in adsorption, which reduces when most sites are

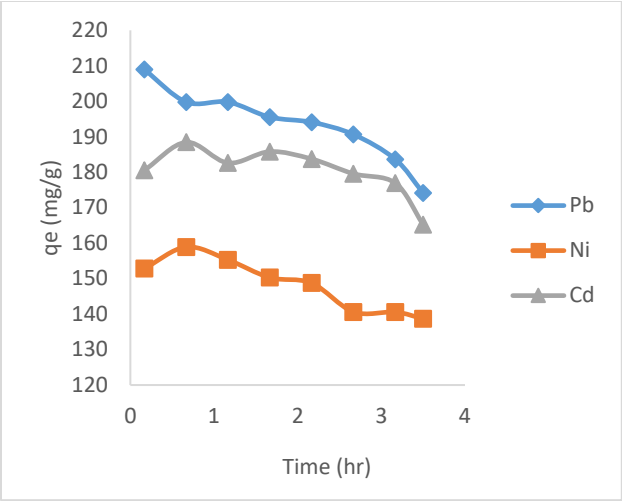

Figure 4d: Effect of time on the adsorption of heavy metal ions on Kaolinite at equilibrium

occupied as the period of contact becomes longer. Similar findings have been reported (Omidi-Khaniabadi *et al.*, 2017; Mohamed *et al.*, 2019).

In general, the kaolinite mineral was found to perform moderately in the adsorption of the three heavy metal ions with 65% of Pb^{2+}, 60% of Ni^{2+} and 57% of Cd^{2+} adsorbed thus the order was Pb^{2+} > Ni^{2+} > Cd^{2+}. The adsorption of heavy metals proceeds through two different mechanisms: ion exchange and complexation. If the former is the primary mechanism, the uptake of the investigated heavy metal ions should vary directly with the ionic radii, the decreasing order of which is Pb > Cd > Ni (Chao & Chang, 2012). If complexation was the case, many factors come into consideration, such as the properties of the metals, the pH of the solution and the functional groups present in the adsorbent (Chao & Chang, 2012; Saxena *et al.*, 2017). Ni^{2+} ions generally exhibit a relatively higher potential to form such complexes, while Pb^{2+} and Cd^{2+} generate relatively higher adsorption amounts through the ion exchange. The order found in the study suggests that the adsorption process was a combination of both mechanisms. In addition, the order could still be explained in terms of the hydrated radii of the ions (Pb^{2+} = 0.401 nm, Ni^{2+} = 0.404 nm and Cd^{2+} = 0.426 nm) and hydration energy (Pb^{2+}= -1481 kJ/mol, Cd^{2+} = -1807 kJ/mol, Ni^{2+} = -2106 kJ/mol) (Mobasherpour *et al.*, 2012).

Adsorption isotherms for adsorption of heavy metals on R-K

The experimental data obtained from the study of the effect of initial concentration at equilibrium time were fitted into Langmuir, Freundlich, and Dubinin Radushkevic (DBR) isotherm equations. The plots are contained in Figures 5a-c, and the parameters' summary is presented in Table 2.

It is apparent from Table 2 that the Langmuir isotherm gave the best fit for all three heavy metals with the highest correlation coefficients of 0.9927,0.9962, and 0.9992 for Pb2+, Ni2+ and Cd2+, respectively. The maximum adsorption capacities for the heavy metals were determined to be 263.16 mg/g, 126.58 mg/g and 109.89 mg/g for Pb^{2+}, Ni^{2+}, and Cd^{2+}, respectively. These values indicate the high adsorption capacity of the clay for the metals. Similar findings have been reported previously (Hai *et al.*, 2015; Yin *et al.*, 2018; Kakaei et al., 2020; Malima *et al.*, 2021).

Kinetics of adsorption of heavy metals on R-K

The data obtained from the time variation at the optimum initial concentrations of the respective heavy metal ions was fitted in three different kinetic models viz pseudo-first order, pseudo-second order and Elovich models as displayed in Figures 6a-c. As shown in Figure 6a-c, only the pseudo-second-order gave the best fit for all the metals. The values of all the parameters are displayed in Table 3.

The high correlation coefficients obtained from the pseudo-second-order model (0.9942 for Pb, 0.9721 for Ni and 0.9628 for Cd) indicate its good fit to the data. The q_e values (238.10 mg/g, 169.50 mg./g and 147.06 mg/g for Pb, Ni and Cd, respectively) derived from the model are in good agreement with q_{exp} (250.00 mg/g, 179.58 mg./g and 155.31 mg/g for Pb, Ni and Cd respectively) values obtained from the experiments.

The major assumption of the pseudo-second-order model is that two reactions are occurring simultaneously: a fast reaction that attains equilibrium rapidly and a much slower second one whose

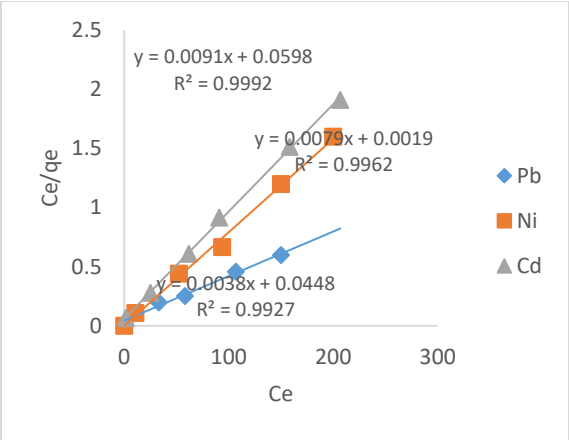

Figure 5a: Langmuir isotherm for the adsorption of heavy metal ions

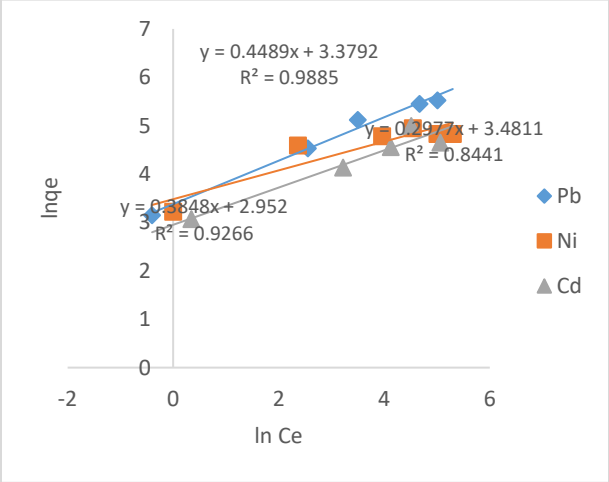

Figure 5b: Freundlich isotherm for the adsorption of heavy metal ions

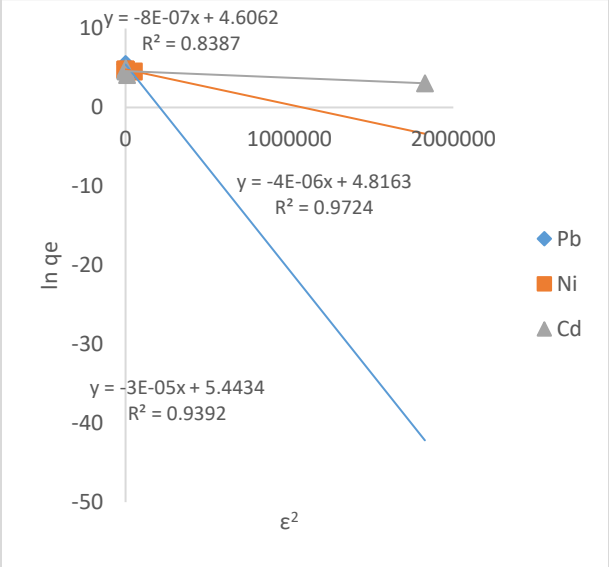

Figure 5c: DBR isotherm for the adsorption of heavy metal ions

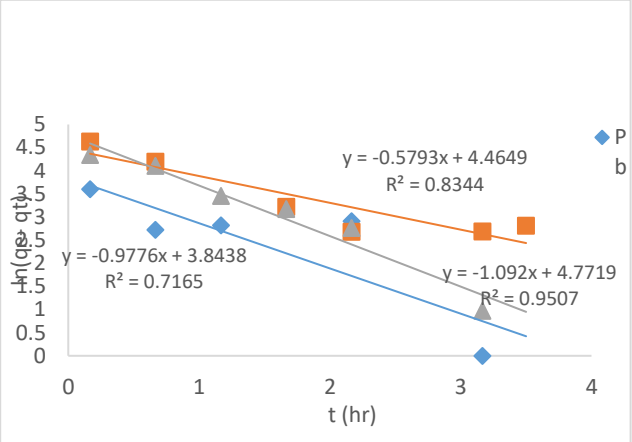

Figure 6a: Pseudo-first order kinetic plots for adsorption of heavy metal ions on R-K

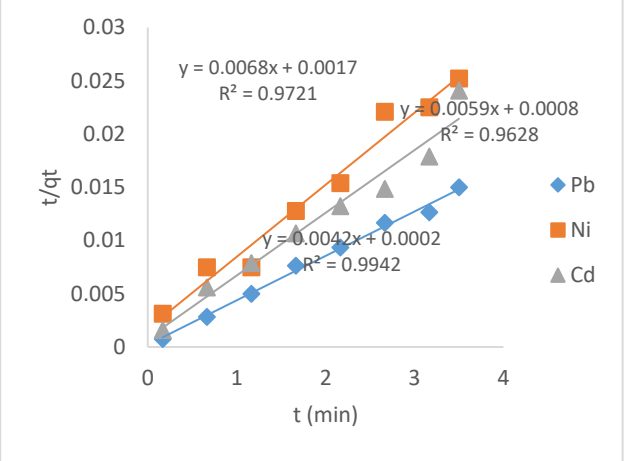

Figure 6b: Pseudo-second order kinetic plots for adsorption of heavy metal ions on R-K

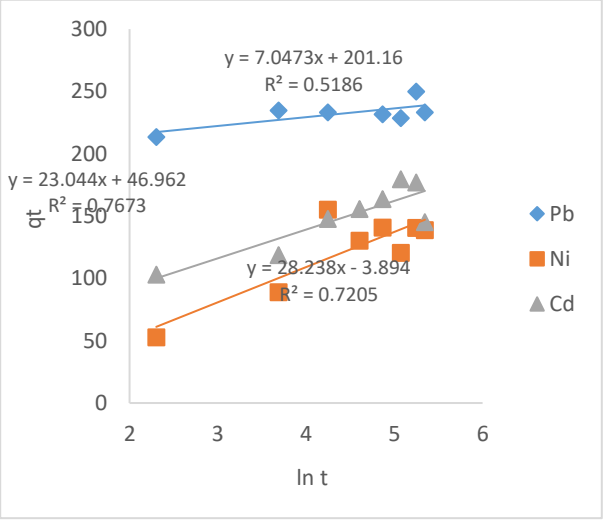

Figure 6c: Elovich kinetic plots for adsorption of heavy metal ions on Kaolinite mineral

Table 2 Isotherm parameters of adsorption of heavy metal ions on Kaolinite mineral

Isotherm models	Kaolinite Clay Pb^{2+}	Ni^{2+}	Cd^{2+}
Langmuir model			
q_L (mg/g)	263.16	126.58	109.89
K_L (L/mg)	0.085	4.158	0.152
R^2	0.9927	0.9962	0.9992
Freundlich model			
K_F $(mg/g)(mg/L)^{1/n}$	29.35	32.50	19.14
N	2.23	3.36	2.60
R^2	0.9885	0.8441	0.9266
DBR model			
q_m (mg/g)	231.23	123.51	100.103
β $(mol^2)(kJ^2)$	3.0 X 10-5	4.0 X 10-5	8.0 X 10-7
E (kJ/mol)	0.12	0.35	0.79
R^2	0.9392	0.9724	0.8387

Table 3: Kinetic parameters of adsorption of heavy metal ions on kaolinite mineral

Kinetic models	Kaolinite Clay Pb^{2+}	Ni^{2+}	Cd^{2+}
q_{exp} (mg/g)	250.00	179.58	155.31
Pseudo-first order model			
$q_{e\ cal}$(mg/g)	46.70	86.91	118.14
$k_1(min^{-1})$	0.9776	0.5793	1.092
R^2	0.7165	0.8344	0.9507
Pseudo-second order model			
$q_{e\ cal}$(mg/g)	238.10	169.50	147.06
k_2 (min^{-1})	0.0882	0.0272	0.004
R^2	0.9942	0.9721	0.9628
Elovich model			
α (mg/gmin)	1.76E+13	24.60056	176.8555
β (gmg^{-1})	0.142	0.035413	0.043395
R^2	0.5186	0.7205	0.7673

.

likely mechanism is:
Clay + M(II) = Clay----M(II)

For such reaction as above, the amount of M(II) ions present in the solution and the number of adsorption sites on the clay surface are considered to determine the kinetics (Meneguin *et al.*, 2017; Yin *et al.*, 2018; Chai *et al.*, 2020). Previous reports of the adsorption of the studied metal ions following pseudo-second order kinetic model have been documented severally (Galindo *et al.*, 2013; Krika *et al.*, 2016; Maged *et al.*, 2020 and Kakaei *et al.*, 2020).

Thermodynamics of adsorption of heavy metals on kaolinite mineral

The Vant Hoff's plots for the adsorption of the three heavy metal ions on the clay are shown in Figures 7a-c and the thermodynamic parameters obtained are presented in Table 4.

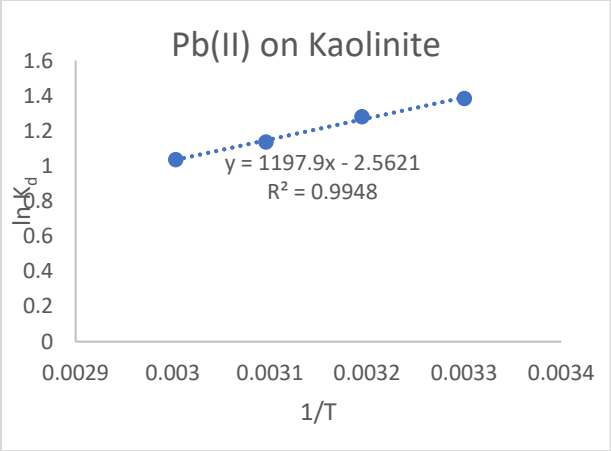

Figure 7a: Vant Hoff plot for the adsorption of Pb^{2+} ions on Kaolinite mineral

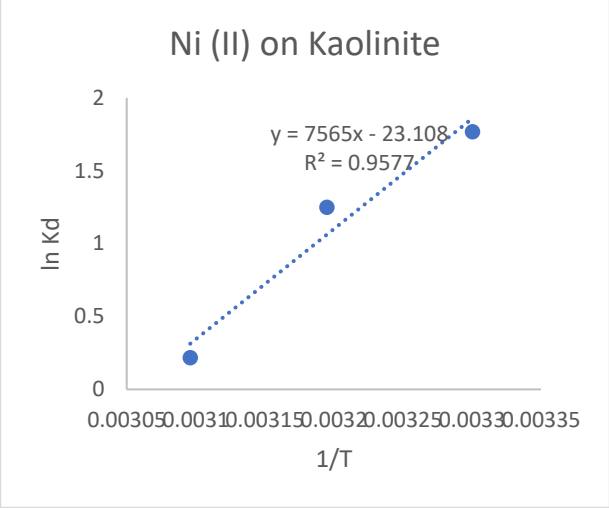

Figure 7b: Vant Hoff plot for the adsorption of Ni^{2+} ions on Kaolinite mineral

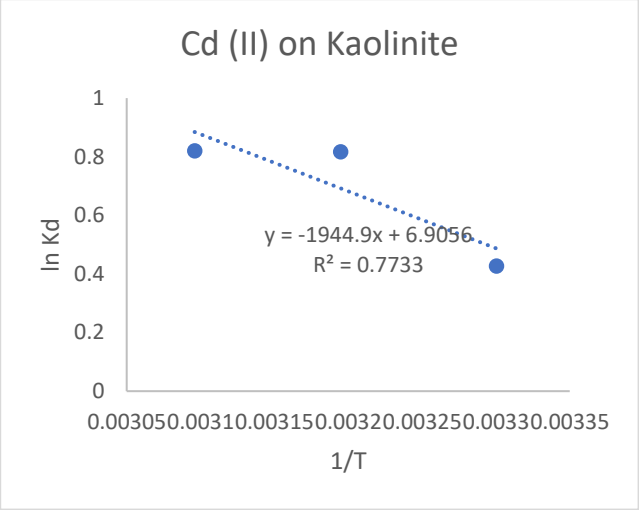

Figure 7c: Vant Hoff plot for the adsorption of Cd^{2+} ions on Kaolinite mineral

Table 4: Thermodynamic parameters of the adsorption of heavy metal ions on Kaolinite mineral

Metal ion	ΔH (kJ/mol)	ΔS (J/mol)	ΔG (kJ/mol)			
			303K	313K	323K	333K
Pb^{2+}	-9.96	-21.30	-3.49	-3.33	-3.05	-2.87
Ni^{2+}	-62.98	-192.12	-1.94	-3.25	-0.58	0.22
Cd^{2+}	16.17	57.41	-1.08	-2.12	-2.20	-2.01

It can be observed from Table 4 that ΔG values are negative for all the heavy metals, which indicates spontaneous adsorption processes at the four different temperatures except for Ni^{2+} at 333K (Malima *et al.*, 2020). The positive value suggests that the adsorption was not favourable for Ni^{2+} at this temperature (El-Naggar *et al.*, 2018). For Pb^{2+} and Ni^{2+} ions, the ΔG values increased from (-3.49 - 2.87 kJ/mol) and (-1.94 – 0.22 kJ/mol), respectively, which implies that there was more affinity between the adsorbent surface and the ions at lower than elevated temperatures while the converse is the case for Cd^{2+} ions whose ΔG values decreased from (-1.08 - -2.01 kJ/mol) (Eba et al., 2013). However, all the ΔG values obtained are lower than -5kJ/mol, indicating that the adsorption process was physisorption (Mnasri-Ghnimi & Srasra, 2019). The adsorption process was exothermic for Pb^{2+} and Ni^{2+} with ΔH values of -9.96 kJ/mol and -62.98 kJ/mol, respectively, while it was endothermic for Cd2+ with ΔH value of 16.17 kJ/mol. The ΔS values were also negative for Pb^{2+}(-21.30 J/mol) and Ni^{2+} (-192.12 J/mol), suggesting that there was a decrease in randomness at the solid-liquid interface, which could be because of the fixation of the metal ions on the surface of the adsorbent. However, a positive value was obtained for Cd^{2+}, which indicates an increase in randomness at the interface and good affinity between the metal ion and the adsorbent surface (Akpomie & Dawodu, 2016; Rao & Khan, 2017).

Desorption studies

Desorption analyses of the three heavy metal ions on the clay mineral were carried out in de-ionized water, 0.5M NaOH and 0.5M HCl. The results are presented in Figure 8. The average percentages of the metals adsorbed on the clay before desorption experiments were carried out were found to be (Pb^{2+} (60%), Ni^{2+} (50%) and Cd^{2+} (47%)). The acidic medium was found to have the most amounts of the adsorbents. Similar findings where HCl was found to desorb heavy metal ions from spent adsorbents have been reported (Adekola *et al.*, 2016; Gebretsadik *et al.*, 2020). appropriate for the removal of all the metals on the clay, as can be observed in Figure 8. The percentage removal from was 78%, 88%, and 95% (HCl), 20.3%, 22% and 25% (NaOH) and 21.55%, 30.47% and 48.3% (De-ionized water) for Cd, Ni and Pb respectively. Pb was found to be most desorbed probably because it was the most adsorbed out of all the metals thus it has the highest

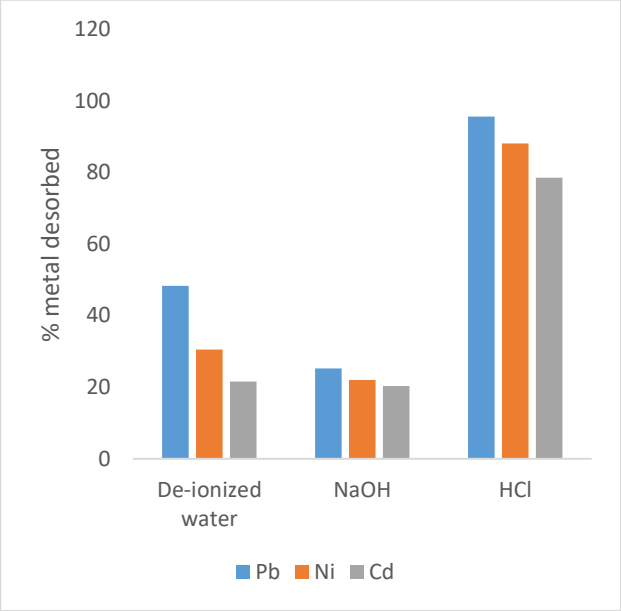

Figure 8: Desorption studies on Kaolinite mineral

Effect of acid activation on the adsorption of heavy metals on kaolinite mineral

As can be observed from Figure 9, the acid-activated clays were able to adsorb more of the heavy metal ions from their respective aqueous solutions than the raw form of the clay. For instance, the quantities of Pb ions adsorbed were A-K; 375 mg/g, N-K; 475 mg/g, O-K; 375 mg/g, P-K; 425 mg/g and S-K; 450 mg/g as opposed to 383.5 mg/g obtained on the raw mineral, R-K. The order of performance was N-K > S-K > P-K > A-K = O-K > R-K. The order seems to be related to the surface areas of the clay samples with the highest values exhibited by N-K and S-K.

Although, O-K has a higher surface area than P-K, the micropore and total pore volumes are higher in P-K, and this could be responsible for the higher performance in P-K compared with O-K. Acetic acid activated clay, A-K has the lowest surface area of all the clays but the removal of Pb^{2+} ions was found to be of the same magnitude as that of O-K which can be because of the higher pore sizes in A-K that could easily trap the metal ions.

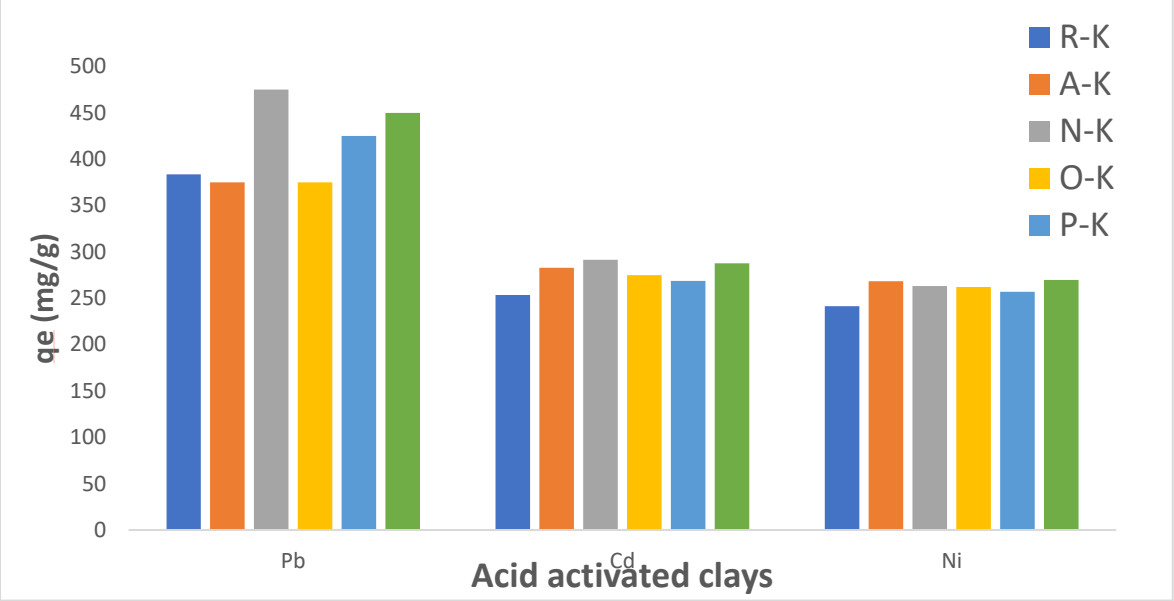

Figure 9: Adsorption of the three heavy metals on acid-activated kaolinite

For Ni^{2+} ions, the order was found to be proportional to the surface area viz N-K (291 mg/g) > S-K (287.5 mg/g) > A-K (282.81 mg/g) > O-K (275 mg/g) > P-K (268.75 mg/g) > R-K (253.45 mg/g) except for A-K for which explanation has already been given. The adsorption of Cd^{2+} ions was almost the same on S-K (269.69 mg/g) > A-K (268.41 mg/g) > N-K (263.27 mg/g) > O-K (261.99 mg/g), but differ for P-K (256.85 mg/g) and R-K (241.45 mg/g). In this instance also, the removal was closely related to the surface areas of the clays with that of A-K being an exception to the rule. In general, the acid-activated clays were better at removing the three heavy metal ions than the raw form of the clay. Similar findings have been reported where the acid-modified clays were better at removing heavy metal ions than the raw form (Khalfa et al., 2016; Bennour, 2017; Dim et al., 2021).

Conclusion

The adsorption potentials of a Nigerian Kaolinite in its raw and acid-activated forms have been successfully investigated. Acid-activated clays were prepared from the clay mineral using inorganic and organic acids. The characterization techniques used in the study confirmed the clay to be 1:1 Kaolinite mineral as well as the changes that occurred in its properties after modification with the acids. The surface area of the clay minerals was significantly increased in the strong acids-activated Kaolinite clays. Adsorption studies of three heavy metal ions were also successfully carried out on the raw clay minerals. The influence of operating conditions viz, pH, initial metal concentration, temperature and time were found to vary for each metal. The Langmuir isotherm correlated best to the adsorption for the three heavy metal ions, while the Pseudo second-order model was the best for the kinetics.

The acid-activated clays were more efficient than the raw form in adsorbing the heavy metal ions from aqueous solutions, and these results confirm the viability of clay minerals as suitable adsorbents for the remediation of waters polluted with heavy metals. In addition, acid activation with dilute acids increases the adsorption potentials of the mineral, and for best results, dilute strong mineral acids are recommended, but weaker acids, as well as organic acids, can also be utilized.

References

Abechi, E., Gimba, C., Uzairu , A., & Kagbu , J. (2011). Kinetics of adsorption of methylene blue onto activated carbon prepared from palm kernel shell. *Archives of Applied Science Research, 3*(1), 154-164.

Adekola, F. A., Hodonou, D. S. S. & Adegoke, H. I. (2016). Thermodynamic and Kinetic Studies of Biosorption of Iron and Manganese from Aqueous Medium Using Rice Husk Ash, *Applied Water Sciences*, 6, 319–330

Ahmadi, A., Foroutan, R., Esmaeili, H. & Tamjidi, S. (2020). The role of bentonite clay and bentonite clay@$MnFe_2O_4$ composite and their physico-chemical properties on the removal of Cr(III) and Cr(VI) from aqueous media. *Environmental Science and Pollution Research*, 27 (12), 14044-14057

Akpomie, K. G. & Dawodu, F. (2016). Acid-modified montmorillonite for sorption of heavy metals from automobile effluent. *Beni - Suef University Journal of Basic and Applied Sciences, 5*, 1–12.

Al-Anber, M. A. (2011). Thermodynamics Approach in the Adsorption of Heavy Metals. In J. M. PirajÃ¡n (Ed.), *Thermodynamics - Interaction Studies - Solids, Liquids and Gases*. Shanghai, China: In Tech. pp. 737-764

Alshameri, A., Hea, H., Zhua, H., Xic, Y., Zhua, R., Maa, L. & Tao, Q. (2018). Adsorption of ammonium by different natural clay minerals: Characterization, kinetics and adsorption isotherms. *Applied clay Science*, 159,83-93

Aziz, K. H. H., Mustafa, F. S., Omer, K. M., Hama, S., Hamaraw, R. F., & Rahman, K. O. (2023). Heavy metal pollution in the aquatic environment: efficient and low-cost removal approaches to eliminate their toxicity: a review, *RSC Advances*, 13(26): 17595–17610.

Bahl, A., Bahl, B. S. & Tuli, G. D. (2012). Essentials of physical chemistry, S. Chand, New Delhi, pp 303-860.

Balali-Mood M., Naseri K., Tahergorabi Z., Khazdair M. R., & Sadeghi M. (2021) Toxic Mechanisms of Five Heavy Metals: Mercury, Lead, Chromium, Cadmium, and Arsenic. *Frontiers in Pharmacology*, 12 (643972) 1-18

Bennour, H. A. M. (2017) Effect of Acid Activation on Adsorption of Iron and Manganese Using Libyan Bentonite Clay, Chemical Science Transactions, 6, (2)**,** 209-218

Berihun, D. & Solomon, Y. (2017). Assessment of the Physicochemical and Heavy Metal Concentration from Effluents of Paint Industry in Addis Ababa, Ethiopia. *International Journal of Waste Resources, 7*(4), 1-5.

Bertagnolli, C. & Carlos da Silva, M. G. (2012). Characterization of Brazillian Bentonite Organoclays as Sorbents of Petroleum-derived Fuels. *Materials Research*, 15, (2), 253-259

Boparai, H. K., Joseph, M. & O'Carroll, D. (2011). Kinetics and thermodynamics of cadmium ion removal by adsorption onto nano zerovalent iron particles. *Journal of HazardousMaterials, 186*(1), 458-465

Budash, Y., Plavan, V., Tarasenko, N., Ishchenko, O. & Koliada, M. (2023). Effect of Acid Modification on Porous Structure and Adsorption Properties of Different Type Ukrainian Clays for Water Purification Technologies. *Journal of Ecological Engineering*, 24, (5), 210–221

Bukalo, N. N., Ekosse, G. E., Odiyo, J. O. & Ogola, J. S. (2017). Fourier Transform Infrared Spectroscopy of Clay Size Fraction of Cretaceous-Tertiary Kaolins in the Douala Sub-Basin, Cameroon. *Open Geosciences*, 9, 407–418

Chai, J. -B., Au, P. -I., Mubarak, N. M., Khalid, M., Ng, W. P. -Q., Jagadish, P., Walvekar, R., & Abdullah, E. C. (2020). Adsorption of heavy metal from industrial wastewater onto low-cost Malaysian kaolin clay–based adsorbent. *Environmental Science and Pollution Research*, 27, (12), 13949 – 13962

Chao, H. -P., & Chang, C. -C. (2012) Adsorption of copper (II), cadmium (II), nickel (II) and lead(II) from aqueous solution using biosorbents, *Adsorption*, 18, 395–401

Chen, M., Yang, T., Han, J., Zhang, Y., Zhao, L., Zhao, J., Li, R., Huang, Y., Gu, Z., & Wu, J. The Application of Mineral Kaolinite for Environment Decontamination: A Review. *Catalysts*, 2023, 13 (123), 1-17

Dim, P. E., Mustapha, L. S., Termtanun, M., Okafor, J. O. (2021) Adsorption of chromium (VI) and iron (III) ions onto acid-modified kaolinite: Isotherm, kinetics and thermodynamics studies, *Arabian Journal of Chemistry*,14, (103064), 1-14

Do, D. D. (1998). Adsorption Analysis: Equilibria and Kinetics; Series on Chemical Engineering,

Vol. 2, Imperial College Press, London. pp 7-101

Eba, F., Ndong Nlo, J., Ondo, J., Andeme Eyi, P. & Nsi‑Emvo, E. (2013) Batch experiments on the removal of U(VI) ions in aqueous solutions by adsorption onto a natural clay surface, *Journal of Environment and Earth Science*, 3, (1), 11-23

El-Naggar, I. M., Ahmed, S. A., Shehata, N., Sheneshen, E. S., Fathy, M., & Shehata, A. (2019). A novel approach for the removal of lead (II) ion from wastewater using Kaolinite/Smectite natural composite adsorbent. *Applied Water Science*, 9, (7), 1-13

Elsheikh, M. A., Muchaonyerwa, P., Johan, E., Matsue, N. & Henmi, T. (2018) Mutual Adsorption of Lead and Phosphorus onto Selected Soil Clay Minerals, *Advances in Chemical Engineering and Science*, 8, 67-81

Emam A.A., Ismail L.E.M., Abdelkhalek M.A., (2016). Adsorption study of some heavy metal ions on modified kaolinite. *International journal of Advancement in Engineering Technology, Management and Applied Science.* 3(7):152-163.

Es-said, A., Nafai, H., Lamzougui, G., Bouhaouss, A. & Bchitou, R. (2021) Comparative adsorption studies of cadmium ions on phosphogypsum and natural clay, *Scientific African*, 13, (e00960), 1-10

Ewere, E. E., Omoigberale, M. O., Bamawo, O. E. & Erhunmwunse, N. O. (2014). Physio-Chemical Analysis of Industrial Effluents in parts of Edo States Nigeria. *Journal of Applied Sciences and Environmental Management, 18*(2), 267-272.

Fernandes, J. V., Rodrigues, A. M., Menezes, R. R., & Neves, G. A. (2020). Adsorption of Anionic Dye on the Acid-Functionalized Bentonite, *Materials*, 13 (3600), 1-19

Foo, K. Y. and Hameed, B. H. (2010). Insights in to the modeling of adsorption isotherm systems. *Chemical Engineering Journal*, 156, 2–10

Galindo, L. S. G., Neto, A. F., da Silva, M. G. C. & Vieira, M. G. A. (2013) Removal of Cadmium (II) and Lead(II) Ions from Aqueous Phase on Sodic Bentonite, *Materials Research*,16, (2), 515-527

Gebretsadik, H., Gebrekidan, A. & Demlie, L. (2020). Removal of heavy metals from aqueous solutions using *Eucalyptus Camaldulensis*: An alternate lowcost adsorbent, *Cogent Chemistry*, 6, (1), 1-16

Hai, Y., Li, X., Wua,, H., Zhao, S., Deligeer, W. & Asuha, S. (2015) Modification of acid-activated kaolinite with TiO2 and its use for the removal of azo dyes, *Applied Clay Science*, 114, 558–567

Hamdaoui, O. & Naffrechoux, E. (2007). Modeling of adsorption isotherms of phenol and. *Journal of Hazardous Materials 147*, 381–394.

Ho, Y. S. & Mckay, G. (1998). Sorption of dye from aqueous solution by peat. *Chemical Engineering Journal*, 115-124

Hooshiar, A., Uhlik, P., Ivey, D. G., Liu, Q. & Etsell, T. H. (2012) Clay minerals in nonaqueous extraction of bitumen from Alberta oil sands Part 2. Characterization of clay minerals, *Fuel Processing Technology*, 96, 183-194

Huang, X., Zhao, H., Zhang, G., Li, J., Yang, Y. & Ji, P. (2020) Potential of removing Cd(II) and Pb(II) from contaminated water using a newly modified fly ash, *Chemosphere* 242, (125148), 1-10

Ihekweme, G. O., Shondo, J. N., Orisekeh, K. I., Kalu-Uka, G. M., Nwuzor, i. C. & Onwualu, A. P. (2020). Characterization of certain Nigerian clay minerals for water purification and other industrial applications, *Heliyon* ,6, e03783, 1-11

Kakaei, S., Khameneh, E. S., Hosseini, M. H. & Moharreri, M. M. (2020) A modified ionic liquid clay to remove heavy metals from water: investigating its catalytic activity *International Journal of Environmental Science and Technology*, 17, 2043–2058

Khalfa, L., Sdiri, A., Bagane, M., & Cervera, M. L. (2020). Multi-element modeling of heavy metals competitive removal from aqueous solution by raw and activated clay from the Aleg formation (Southern Tunisia). *International Journal of Environmental Science and Technology,* 17, 2123–2140

Khan, M. I., Almesfer, M. K., Danish, M., Ali, I. H., Shoukry, H., Patel, R., Gardy, J., Nizami, A. S.

& Rehan, M. (2019). Potential of Saudi natural clay as an effective adsorbent in heavy metals removal from wastewater, *Desalination and Water Treatment,* 158, 140–151

Krika, F., Azzouz, N. & Ncibi, M. C. (2016). Adsorptive removal of cadmium from aqueous solution by cork biomass: Equilibrium, dynamic and thermodynamic studies. Arabian Journal of Chemistry, 9, (2), 1077-1083

Kumar, A. & Lingfa, P. (2020). Sodium bentonite and kaolin clays: Comparative study on their FT-IR, XRF, and XRD, *Materials Today: Proceedings* ,22, 737-742

Kumar, S., Panda, A.K. & Singh, R. K. (2013). Preparation and Characterization of Acids and Alkali Treated Kaolin Clay. *Bulletin of Chemical Reaction Engineering & Catalysis*, 8 (1), 61 – 69

Lawal J.A., Odebunmi E.O., & Adekola F.A., (2020). Adsorption of Fe^{2+}, Pb^{2+}, Zn^{2+} and Cr^{6+} ions from aqueous solutions using natural, ammonium oxalate and sodium hydroxide modified kaolinite clay. *Ife Journal of Science* 22(3): 001-023.

Levine, I. N. (2009). Physical chemistry, Mc-Graw Hill International Edition, Mc-Graw Hill, New York. pp 161-575

Li, T., Huang, X., Wang, Q. & Yang, G. (2020). Adsorption of metal ions at kaolinite surfaces: Ion-specific effects, and impacts of charge source and hydroxide formation. *Applied Clay Science*, 194, (105706), 1-10

Likita, M. B., Nura, G. K., Nuhu, C. D. & Isah, S. D. (2016). Physico-Chemical Characterization of Industrial Effluents in Minna Niger State, Nigeria. *International Journal of Modern Analytical and Separation Sciences, 5*(1), 12-19.

Maged, A., Ismael, I. S., Kharbish, S., Sarkar, B., Peräniemi, S. & Bhatnagar, A. (2020) Enhanced interlayer trapping of Pb (II) ions within kaolinite layers: intercalation, characterization, and sorption studies. *Environmental Science and Pollution Research* 27**,** 1870–1887

Malima, N. M., Owonubi, · S. J., Lugwisha, E. H. & Mwakaboko, A. S. (2021) Thermodynamic, isothermal, and kinetic studies of heavy metals adsorption by chemically modified Tanzanian Malangali kaolin clay, *International Journal of Environmental Science and Technology*, 18, (10), 3153-3168.

Meneguin, J. G., Moisés, M. P., Karchiyappana, T., Fariaa, S. H. B., Gimenes, M. L., de Barros, M. S. D. & Venkatachalam, S. (2017) Preparation and characterization of calcium treated bentonite clay and its application for the removal of lead and cadmium ions: Adsorption and thermodynamic modelling, *Process Safety and Environmental Protection*, 1 1 1, 244–252

Mnasri-Ghnimi, S. & Srasra, N. (2019) Removal of heavy metals from aqueous solutions by adsorption using single and mixed pillared clays, *Applied Clay Science*, 179, (105151), 1-17

Mobasherpour, I., Salahi, E., & Pazouki, M. (2012) Comparative of the removal of Pb^{2+}, Cd^{2+} and Ni^{2+} by nano crystallite hydroxyapatite from aqueous solutions: Adsorption isotherm study, *Arabian Journal of Chemistry*, 5, 439-446

Mohamed, H. S., Soliman, N. K., Abdelrheem, D. A., Ramadan, A. A., Elghandour, A. H. & Ahmed, S. A. (2019). Adsorption of Cd^{2+} and Cr^{3+} ions from aqueous solutions by using residue of *Padina gymnospora* waste as promising low-cost adsorbent. *Heliyon*, 5, e01287, 1-32

Moretti, L. Natali, S., Tiberi, A. & D'Andrea, A. (2020). Proposal for a Methodology Based on XRD and SEM-EDS to Monitor Effects of Lime-Treatment on Clayey Soils, *Applied Sciences* 10, 2569, 1-17

Mudzielwana, R., Gitari, M. W. & Ndungu, P. (2019) Performance evaluation of surfactant modified kaolin clay in As(III) and As(V) adsorption from groundwater: adsorption kinetics, isotherms and thermodynamics, *Heliyon*, e02756, 1-13

Nordin, N. A., Abdul Rahman, N. & Abdullah, A. (2020) Effective Removal of Pb(II) Ions by Electrospun PAN/Sago Lignin-Based Activated Carbon Nanofibers, *Molecules* , 25, (3081), 1-21

Novakovic., T., Rozi˘c´, L., Petrovic´, S. & Rosic´, A. (2008). Synthesis characterization of acid-activated Serbian smectite clays obtained by

statistically designed experiments, *Chemical Engineering Journa*l, 137, 436–442

Ogbu, I. C., Akpomie, K. G., Osunkunle, A. A., & Eze, S. I. (2019). Sawdust-kaolinite composite as efficient sorbent for heavy metal ions. *Bangladesh Journal of Scientific and. Industrial Research,* 54, (1), 99-110

Omer, O. S., Hussein, M. A., Hussein, B. H. & Mgaidi, A. (2018). Adsorption thermodynamics of cationic dyes (methylene blue and crystal violet) to a natural clay mineral from aqueous solution between 293.15 and 323.15 K. *Arabian Journal of Chemistry, 11*, 615–623.

Omidi Khaniabadi, Y., Basiri, H., Nourmoradi, H., Mohammadi, M. J., Yari, A. R., Sadeghi, S., & Amrane, A. (2017). Adsorption of Congo Red Dye from Aqueous Solutions by Montmorillonite as a Low-cost Adsorbent. *DE GRUYTER: International Journal of Chemical Reactor Engineering*, 20160203, 1-11

Özcan, A. S. & Özcan, A. (2004). Adsorption of acid dyes from aqueous solutions onto acid-activated bentonite. *Journal of Colloid and Interface Science, 276*, 39–46.

Ozdes, D., Duran, C. & Senturk, H. B. (2011). Adsorptive removal of Cd(II) and Pb(II) ions from aqueous solutions by using Turkish illitic clay. *Journal of Environmental Management*, 92, 3082-3090.

Panda, A. K., Mishra, B. G., Mishra, D. K. & Singh, R. K. (2010). Effect of sulphuric acid treatment on the physico-chemical characteristics of kaolin clay. *Colloids and Surfaces A: Physicochemical and Engineering Aspects*, 363, 98–104

Pathania, D., Sharma, S. & Singh, P. (2017). Removal of methylene blue by adsorption onto activated carbon developed from Ficus carica bast. *Arabian Journal of Chemistry, 10*, 1445–1451.

Ramachandran, P., Vairamuthu, R. & Ponnusamy, S. (2011). Adsorption Isotherms, Kinetics, Thermodynamics and Desorption Studies of Reactive Orange 16 ob Activated Carbon Derived fron Ananascomosus (L.). *ARPN Journal of Engineering and Applied Sciences, 6*(11), 15-26.

Rao, R. A. K. & Khan, U. (2017) Adsorption studies of Cu(II) on Boston fern (Nephrolepis exaltata Schott cv. Bostoniensis) leaves, *Applied Water Science*, 7, 2051–2061

Sarma, G. K., Sen Gupta, S., & Bhattacharyya, K. G. (2019) Removal of hazardous basic dyes from aqueous solution by adsorption onto kaolinite and acid-treated kaolinite: kinetics, isotherm and mechanistic study, *Springer Nature Applied Sciences*, 1, (211), 1-15

Saxena, A., Bhardwaj, M., Allen, T., Kumar, S. & Sahney, R. (2017) Adsorption of heavy metals from wastewater using agricultural–industrial wastes as biosorbents, *Water Science*, 31, (2), 189-197

Sdiri, A., Higashi, T., Hatta, T., Jamoussi, F. & Tase, N. (2011). Evaluating the adsorptive capacity of montmorillonitic and calcareous clays on the removal of several heavy metals in aqueous systems. *Chemical Engineering Journal*, 172, 37-46

Siyanbola, T., Ajanaku , K. O., James , O. O. & Olugbuyiro, J. A. (2011). Physico-Chemical Characteristics of Industrial Effluents In Lagos State, Nigeria. *G. J. P&A Sc and Tech., I*, 49-54.

Sukpreabprom, H., Arquero , A., Naksata, W., Sooksa, P. & Janhom, S. (2014). Isotherm, Kinetic and Thermodynamic Studies on the Adsorption of Cd (II) and Zn (II) ions from Aqueous Solutions onto Bottom Ash. *International Journal of Environmental Science and Development, 5* (2), 165-170.

Tian, L., Fu1, K., Chen, S., Yao, J. & Bian, L. (2022). Comparison of microscopic adsorption characteristics of Zn(II), Pb(II), and Cu(II) on kaolinite. *Scientific Reports*, 12, (15936), 1-12

Uddin, M. K. (2017). A review on the adsorption of heavy metals by clay minerals, with special focus on the past decade. *Chemical Engineering Journal 308*, 438–462.

Yin, J., Deng, C., Yu, Z., Wang, X. & Xu, G.(2018) Effective Removal of Lead Ions from Aqueous Solution Using Nano Illite/Smectite Clay: Isotherm, Kinetic, and Thermodynamic Modeling of Adsorption, *Water,* 10, (210), 1-13